

## Exfoliated Polymer Nanocomposites by *In Situ* Coprecipitation of Layered Double Hydroxides in a Polymer Matrix

Julien Gaume,<sup>1,2</sup> Sandrine Therias,<sup>1,2</sup> Fabrice Leroux,<sup>1,2</sup> Agnès Rivaton,<sup>1,2</sup> Jean-Luc Gardette<sup>1,2</sup>

<sup>1</sup>Clermont Université, Université Blaise Pascal, Institut de Chimie de Clermont-Ferrand, BP 10448, F-63000 Clermont-Ferrand, France

<sup>2</sup>CNRS, UMR 6296, ICCF, BP 80026, F-63171 Aubiere, France

Correspondence to: S. Therias (E-mail: sandrine.therias@univ-bpclermont.fr) or F. Leroux (E-mail: fabrice.leroux@univ-bpclermont.fr)

**ABSTRACT:** Polyvinylalcohol (PVA) nanocomposites were prepared by a “one step” method based on the coprecipitation of layered double hydroxide (LDH) platelets in the polymer aqueous solution. The PVA/LDH nanocomposites displayed an exfoliated morphology and the concentration of LDH in the nanocomposite was evaluated by IR analysis. Moreover, it was shown that the PVA/LDH nanocomposites had an improved photostability over PVA, which makes this material a good candidate for coating applications. Further optimization will be considered to tune the polymer/LDH properties. © 2012 Wiley Periodicals, Inc. *J. Appl. Polym. Sci.* 129: 1345–1349, 2013

**KEYWORDS:** clay; composites; photochemistry; synthesis and processing; degradation

Received 23 October 2012; accepted 14 November 2012; published online 5 December 2012

DOI: 10.1002/app.38831

### INTRODUCTION

The growing interest in applications for nanocomposite materials in many industrial fields is the driving force for the development of new polymer matrix/nanofiller formulations. Attention has focused on the use of layered silicates, such as smectite clays (montmorillonite), but was recently extended to layered double hydroxides (LDH), known as hydroxide-like compounds. The LDH structure consists of brucite-like sheets, in which the partial substitution of trivalent for divalent cations induces a positive sheet charge that is compensated by anions within interlayer galleries.<sup>1</sup> The general formula of an LDH is  $[M_{1-x}^{2+}M_x^{3+}(\text{OH})_2]^{x+}[(A^{n-})_{x/n}, n\text{H}_2\text{O}]$ . The incorporation of lamellar nanofillers into polymer matrices is commonly performed via three different methods: melt intercalation, intercalation of the polymer from solution and *in situ* intercalative polymerization.<sup>2,3</sup> LDH-type materials have been extensively studied as polymer filler and fire-retardant materials, due to their associated form factor, tuneable composition, and container role.<sup>1,4–7</sup> However, due to their high charge densities, LDH platelets are difficult to exfoliate, in contrast to swelling cationic clays that bear less layer charges. Stacked LDH platelets can be disassembled using chemical procedures that are not used for processing the polymer, such as the use of unfriendly solvents with modified surfactants<sup>8–10</sup> or through the use of LDH platelets composed of nitrates.<sup>11,12</sup> Also worth noting are alkoxide<sup>13</sup> and lactate-intercalated<sup>14,15</sup> LDH platelets that

delaminate in room-temperature water to form stable, translucent colloidal solutions.

The strategy we investigated to obtain exfoliated polymer nanocomposites is based on the *in situ* coprecipitation of the LDH nanofiller directly with the polymer from solution. Instead of mixing the nanoclay with the monomer solution followed by polymerization, the goal is to build the nanofiller platelets in the polymer solution, which allows the platelets to be in the vicinity of the polymer chains. The polymer solution acts as a dispersant medium that prevents the stacking of the generated sheets, which leads to the exfoliated morphology. LDH phases can be prepared using a coprecipitation method from an aqueous solution,<sup>16</sup> which is a method that can be directly applied to water-soluble polymers. Polyvinylalcohol (PVA) was chosen as the polymeric matrix, and the LDH phase was  $[\text{Zn}_2\text{-Al-NO}_3]$ . Blends of PVA and LDH that led to intercalated nanocomposites (i.e., the reference materials) were also prepared by a solution-intercalation of the polymer, which is the most commonly used preparation method of PVA nanocomposites.<sup>17–21</sup>

In this study we report the synthesis of PVA/LDH nanocomposites using a “one step” method, which led to a well-dispersed nanofiller with an exfoliated nanomorphology that was consistent with characterization data from IR spectroscopy, XRD and TEM analyses. The photostability of the PVA/LDH nanocomposites was also investigated and compared with that of PVA/clay nanocomposites.<sup>22</sup>

## EXPERIMENTAL

### Materials

PVA (98% hydrolyzed, weight-average molecular weight  $\approx 16,000 \text{ g}\cdot\text{mol}^{-1}$ ) was purchased from Scientific Polymer Products. Before use, the PVA was purified with methanol in a Soxhlet apparatus for two days.

$\text{Zn}(\text{NO}_3)_2\cdot 6\text{H}_2\text{O}$  and  $\text{Al}(\text{NO}_3)_3\cdot 9\text{H}_2\text{O}$  salts were purchased from Acros and were used as received.

### Preparation of Nanocomposite Films

PVA/LDH nanocomposites were synthesized using a “one-step” coprecipitation method, which was also used for the LDH phase preparation. The total amount of metallic salts was chosen to yield PVA/LDH nanocomposites with 10 wt % filler loading if complete coprecipitation occurred (500 mg of  $[\text{Zn}_2\text{-Al-NO}_3]$  in 4.5088 g of PVA). PVA was dissolved in a 50 mL solution of decarbonated water (prepared under stirring for 3 h at  $80^\circ\text{C}$ ), and then a solution of  $\text{Zn}(\text{NO}_3)_2$  (836 mg) and  $\text{Al}(\text{NO}_3)_3$  (526 mg) (Zn:Al ratio of 2:1) was added dropwise under vigorous stirring. The addition was performed at room temperature under nitrogen and using the addition of NaOH (0.5 M) to maintain a constant pH of 9. The colloid solution was left for 3 h with constant stirring, and then the films were solvent-cast directly from the solution.

Nanocomposites prepared by mixing the PVA aqueous solution (5 wt%) and a suspension of an LDH precursor phase ( $[\text{Zn}_2\text{-Al-NO}_3]$ , previously synthesized<sup>8</sup>) were also prepared at different LDH concentrations (2.5, 5.0, 7.5, 10, and 12.5 wt %). The PVA/LDH solutions were stirred at room temperature overnight and sonicated for 30 min in an ultrasonic bath. Free-standing films were obtained by depositing the PVA/LDH aqueous solutions using an Erichsen Coatmaster 809 MC on a Teflon sheet. After drying the films at room temperature for 1 day and at  $60^\circ\text{C}$  for 3 h, 20–30  $\mu\text{m}$ -thick films were obtained, which were suitable for spectroscopic analysis. In the case of *in-situ* PVA/LDH synthesis, the nanocomposite films were washed by Soxhlet extraction in methanol for 24 h to remove  $\text{NaNO}_3$  and residual unreacted salts.

### Exchange Reaction with Carbonate Anions and Hydrothermal Treatment

To confirm the formation of LDH platelets in the colloid solution resulting from *in situ* coprecipitation synthesis, an exchange reaction of nitrate anions with carbonate anions was performed to build up a  $[\text{Zn-Al-CO}_3]$  LDH phase, that can be easily identified by XRD.

Part of the PVA/LDH colloid solution (20 mL) was placed in a saturated aqueous solution of  $\text{CaCO}_3$  and left under stirring overnight at room temperature.

To increase the size and crystallinity of the materials resulting from the *in situ* coprecipitation synthesis, the colloid solution was placed in a sealed reactor at  $100^\circ\text{C}$  for 5 days under a hydrothermal postsynthesis treatment.

### UV-Visible Irradiation

The UV-visible light irradiation ( $\lambda > 300 \text{ nm}$ ) of the thin films was performed in a SEPAP 12/24 unit, which was designed for

studying polymer photodegradation in artificial ageing with medium-accelerated conditions.<sup>23</sup> The chamber consisted of a square reactor equipped with four medium-pressure mercury lamps (Novalamp RVC 400W) situated vertically at each corner of the chamber. Wavelengths below 300 nm are filtered by the glass envelope of the lamps. In the center of the chamber, the samples are fixed on a 13-cm-diameter rotating carousel that could hold 24 samples. In this set of experiments, the temperature at the surface of the samples was set at  $60^\circ\text{C}$ .

### Characterization Techniques

TEM images were obtained from an aqueous solution of PVA/LDH deposited on a copper grid covered with collodion and carbon film. TEM images were acquired using a Hitachi H-7650 operating with an acceleration voltage of 80 kV.

XRD profiles were obtained with a Siemens Model D500 X-ray diffractometer with a diffracted beam monochromator Cu K $\alpha$  source. Patterns were recorded over the  $2\theta$  range of  $2\text{--}70^\circ$  (or  $1\text{--}5^\circ$  for low angles measurements), in steps of  $0.08^\circ$  (or  $0.04^\circ$ ) with a count time of 4s (or 10 s).

IR spectra were recorded in transmission mode with a Nicolet 6700 Fourier transform infrared (FTIR) spectrophotometer operated with the OMNIC software. The spectra were obtained from 32 scan summations at  $4 \text{ cm}^{-1}$  resolution.

## RESULTS AND DISCUSSION

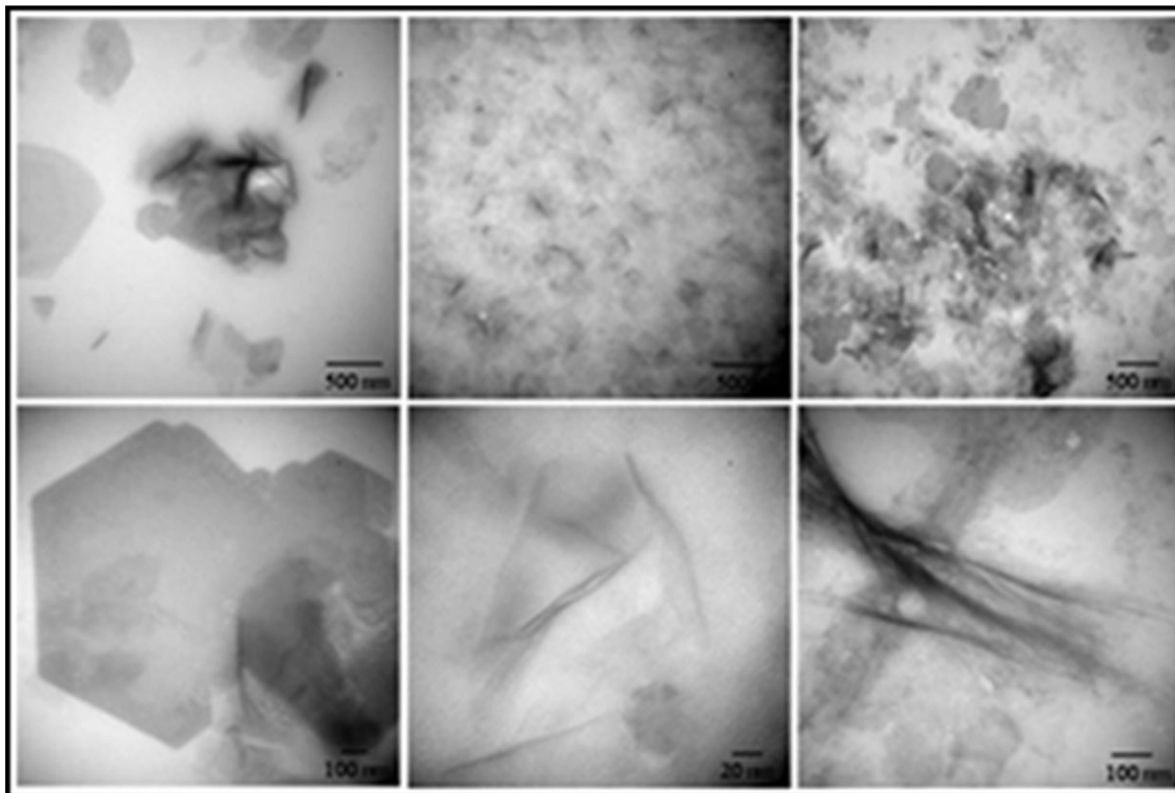
### TEM Characterization

The formation of a layered inorganic structure in the polymer solution by coprecipitation was analyzed by transmission electron microscopy (TEM).

Figure 1(a,d) show the PVA/LDH nanocomposites obtained by blending nanofillers at 2.5 wt % of LDH in an aqueous solution of PVA. The hexagonal platelets of LDH can be clearly observed. Figure 1(b) displays the lower magnification image of the materials obtained after the *in situ* coprecipitation of LDH in an aqueous solution of PVA. A distribution of dark lines can be observed in the micrographs, which represent the global dispersion of inorganic platelets in the polymer matrix. The TEM image at high magnification [Figure 1(e)] reveals the presence of single layers of inorganic materials in the PVA matrix, which correspond to exfoliated LDH nanocomposites. The PVA/LDH nanocomposite was also characterized by TEM after hydrothermal treatment, as shown in Figure 1(c,f) that clearly show a more highly ordered phase with some tactoids of inorganic materials of larger lateral size with sheet stacking.

### X-ray Diffraction Analysis

XRD analyses were required to complement the data from the TEM experiments and to further confirm that the platelets were formed by the “one-step” nanocomposite preparation method corresponding to the LDH exfoliated sheets. The *in situ* synthesis after coprecipitation should lead to the formation of LDH platelets with nitrate as counter ions in the PVA polymer. An exchange reaction with carbonate ions was performed (using a 10-fold excess of  $\text{CaCO}_3$ ) to build up a  $\text{Zn-Al-CO}_3$  phase by stacking the metallic octahedral sheets with carbonate anions.



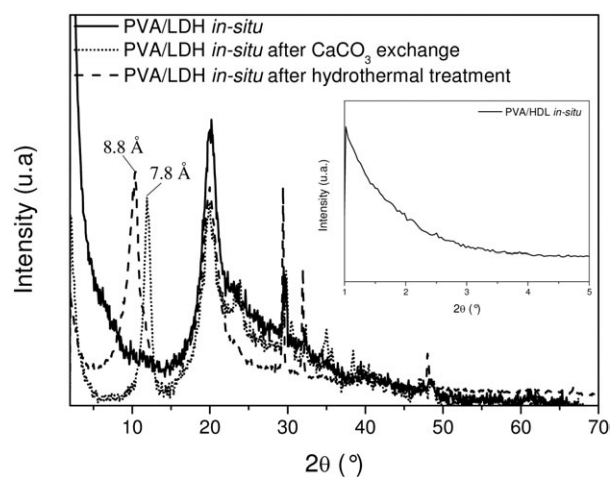
**Figure 1.** TEM images of a solution-blended PVA/LDH 2.5 wt % nanocomposite (a, b), an *in situ* nanocomposite (c, d) and an *in situ* nanocomposite after hydrothermal treatment (e, f).

Figure 2 shows the XRD patterns of the nanocomposite films obtained by the *in situ* coprecipitation method. The XRD pattern of the nanocomposite films after coprecipitation shows no noticeable reflections related to the stacked LDH, even at low angles (Figure 2 insert), which is indicative of a disordered or exfoliated nanostructure within the PVA polymer matrix. Successful anionic exchange reactions replacing nitrate for carbonate ions was performed, as evidenced by the XRD data collected after  $\text{CaCO}_3$  treatment (Figure 2), which show a new diffraction peak corresponding to a (003) reflection of a  $[\text{Zn}_2\text{-Al-CO}_3]$  LDH phase and a  $d$ -spacing value of 7.8 Å. The XRD data support the theory that the carbonate anions are arranged in the interlayer spaces and are in good agreement with the previously reported values for a  $[\text{Zn}_2\text{-Al-CO}_3]$  LDH phase.<sup>24,25</sup> Moreover, the nanocomposite (Figure 2) displays strong reflections with the appearance of a (003) reflection after hydrothermal treatment. The reflection corresponds to a nitrate-containing LDH phase expected at 8.8 Å. The observed stacking properties of the sheets confirm that LDH platelets were formed in the PVA solution using the *in situ* coprecipitation synthesis of the nanocomposite. In the case of hydrothermal treatment, the (001) reflections are characterized by high intensities combined with narrow peak widths, indicating that the LDH phase presents a relatively high crystallinity.

#### Infra-Red Analysis

The evaluation of the amount of the LDH phase formed in the PVA/LDH nanocomposite by the “one-step” coprecipitation

preparation method was performed using transmission IR analysis of the film, as elemental analysis would fail in separating the cation composition contributions from the LDH framework and unreacted cation salt. Comparing the IR spectra of the PVA/LDH blends (at different LDH loadings) and the *in situ* nanocomposite allowed us to calculate the weight percentage of LDH in the polymer.



**Figure 2.** XRD patterns of PVA/LDH films from the *in situ* synthesis after coprecipitation, the exchange reaction with  $\text{CaCO}_3$  and hydrothermal treatment. Insert: A low-angle XRD pattern of a PVA/LDH film obtained from an *in situ* synthesis after coprecipitation.

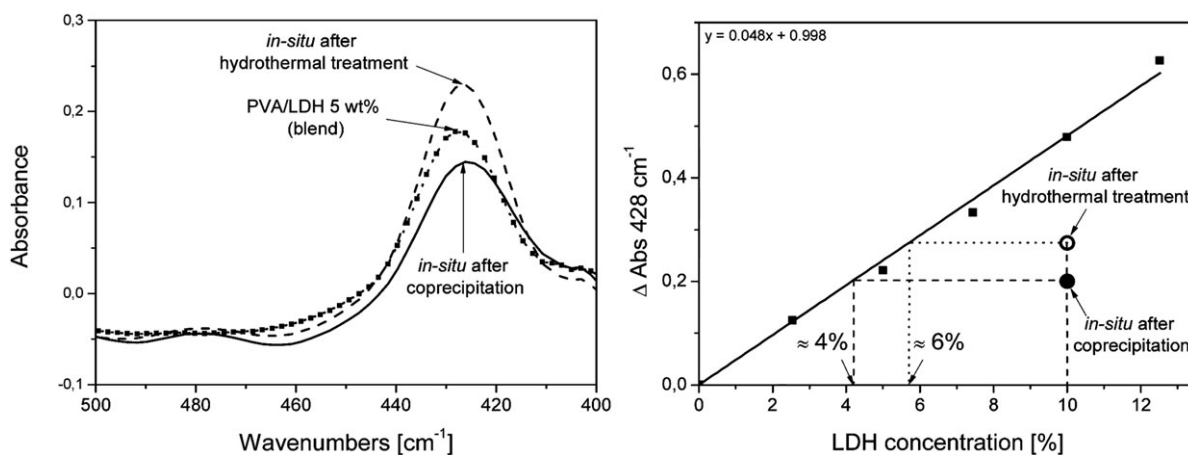


**Figure 3.** (a) IR spectra of PVA/LDH nanocomposites either obtained by *in situ* coprecipitation or by solution blending, and (b) the calibration curve was obtained by plotting the absorbance at  $428\text{ cm}^{-1}$  as a function of the LDH loading and LDH concentration obtained for the *in-situ* PVA/LDH nanocomposite film.

IR spectra of the PVA/LDH blends [Figure 3(a)] display the characteristic vibration bands of the LDH in the PVA/LDH nanocomposite films. Among them, the absorption band at  $428\text{ cm}^{-1}$ , corresponding to a  $\delta_{\text{O-Zn-O}}$  vibration band of LDH hydroxylated sheets, was used to obtain a calibration curve for the amount of LDH in the nanocomposite, by plotting the absorbance at  $428\text{ cm}^{-1}$  as a function of LDH loading [Figure 3(b)]. The IR spectra of the *in situ* nanocomposites (after coprecipitation and after hydrothermal treatment [Figure 3(a)]) show the presence of a characteristic absorption band for LDH at  $428\text{ cm}^{-1}$ . Moreover, the corresponding absorbance can be correlated to a quantity of LDH with the calibration curve. The obtained results for the PVA/LDH nanocomposites prepared by the “one step” method give 4 and 6 wt % loading of LDH for the samples after coprecipitation and hydrothermal treatment, respectively [Figure 3(b)].

#### Photostability of PVA/LDH Nanocomposites

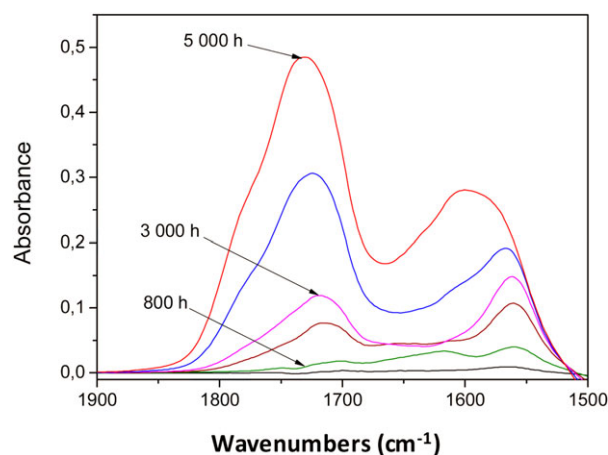
The photochemical behaviour of PVA was investigated in our previous paper.<sup>26</sup> The influence of LDH on the photochemical stability of PVA was evaluated by IR analysis under UV-light irradiation in the presence of oxygen. Photooxidation results in noticeable modifications in the IR spectrum of PVA, with a decrease in C-H groups and the formation of carbonyl photo-products.<sup>26</sup> The subtracted IR spectra (in the carbonyl region) of PVA/LDH nanocomposite films (from the *in situ* preparation) during photooxidation are presented in Figure 4.

Figure 4 shows the formation of new absorption bands with two maxima at  $1735\text{ cm}^{-1}$  and  $1560\text{ cm}^{-1}$ , that shifted to  $1600\text{ cm}^{-1}$  for longer irradiation time. The changes of IR spectra of PVA/LDH under irradiation are different from those observed from pristine PVA. The broad IR absorption band at  $1735\text{ cm}^{-1}$  corresponds to the photoproducts observed in the case of PVA, which were identified as carboxylic acids and among others carboxylic acids of low molecular weight such as acetic, malonic, oxalic, and succinic acids.<sup>26</sup> The IR absorption band at  $1560\text{ cm}^{-1}$  observed in presence of LDH can be attributed to carboxylate forms of some of these acids due to the basic environment of hydroxide platelets of LDH. This peculiar behaviour of

polymer/LDH nanocomposite under photooxidation has already been observed with polypropylene/[Zn-Al-DS] (DS = dodecyl sulphate)<sup>27</sup> and polypropylene/hydroxalite nanocomposites.<sup>28</sup>

To compare the photostability of PVA with or without the presence of LDH, the rates of PVA photooxidation were compared for the different PVA/LDH nanocomposite films and for pristine PVA. The increase in absorbance in the carbonyl domain (measured in the IR spectra) which corresponds to the formation of carboxylic acids (photooxidation products of PVA)<sup>26</sup> was plotted as a function of irradiation time (Figure 5).

Figure 5 shows a lower oxidation rate of PVA in the case of PVA/LDH blends at 5 and 10 wt %. In the case of the *in situ* synthesis, the kinetic curve of the PVA photooxidation is the same as that observed for a pristine PVA film. These results show that LDH improves the photostability of the PVA in nanocomposites, whereas cationic clays, such as montmorillonite, are known to induce a prodegradant effect on polymer photooxidation.<sup>22,29</sup>



**Figure 4.** Subtracted IR spectra (in the carbonyl region) of PVA/LDH nanocomposite film (*in situ* prepared) during photooxidation at  $\lambda > 300\text{ nm}$  and  $60^\circ\text{C}$ . [Color figure can be viewed in the online issue, which is available at [wileyonlinelibrary.com](http://wileyonlinelibrary.com).]

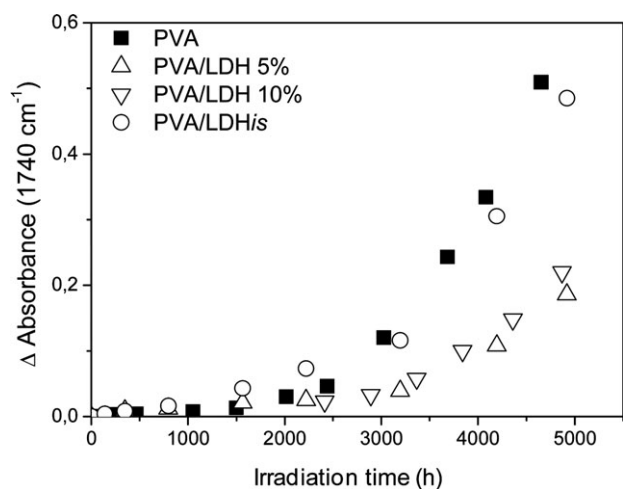


**Figure 5.** Rate of formation of carbonylated product of PVA during photooxidation for pristine PVA, PVA/LDH 5%, PVA/LDH 10%, and PVA/LDH *in situ* nanocomposite films.

## CONCLUSIONS

In conclusion, we achieved an *in situ* preparation of PVA/LDH nanocomposites by a direct coprecipitation method of LDH nanoplatelets within the polymer solution. The concentration of LDH in the nanocomposite obtained by this “one-step” method was evaluated by IR analysis. This new method provides an efficient way to produce exfoliated PVA/LDH nanocomposites. Further optimization will be considered to tune the polymer/LDH properties, such as those regarding the gas barrier and photostability.

## REFERENCES

1. Leroux, F.; Taviot-Gueho, C. *J. Mater. Chem.* **2005**, *15*, 3628.
2. Alexandre, M.; Dubois, P. *Mater. Sci. Eng. R: Rep.* **2000**, *28*, 1.
3. Pavlidou, S.; Papaspyrides, C. D. *Prog. Polym. Sci.* **2008**, *33*, 1119.
4. Leroux, F.; Forano, C.; Prevot, V.; Taviot-Gueho, C. "LDH assemblies and related nanocomposites", *American Scientific Publishers*, **2009**, 42.
5. Pereira, C. M. C.; Herrero, M.; Labajos, F. M.; Marques, A. T.; Rives, V. *Polym. Degrad. Stab.* **2009**, *94*, 939.
6. Chiang, M. F.; Chu, M. Z.; Wu, T. M. *Polym. Degrad. Stab.* **2001**, *96*, 60.
7. Manzi-Nshuti, C.; Songtipya, P.; Manias, E.; Jimenez-Gasco, M. M.; Hossenlopp, J. M.; Wilkie, C. A. *Polymer* **2009**, *50*, 3564.
8. Leroux, F.; Adachi-Pagano, M.; Intissar, M.; Chauviere, S.; Forano, C.; Besse, J. P. *J. Mater. Chem.* **2001**, *11*, 105.
9. Venugopal, B. R.; Shivakumara, C.; Rajamathi, M. *J. Colloid Interface Sci.* **2006**, *294*, 234.
10. Nakagaki, S.; Halma, M.; Bail, A.; Arazaga, G.; Wypych, F. *J. Colloid Interface Sci.* **2005**, *281*, 417.
11. Liu, Z.; Ma, R.; Osada, M.; Iyi, N.; Ebina, Y.; Takada, K.; Sasaki, T. *J. Am. Chem. Soc.* **2006**, *128*, 4872.
12. Wu, Q.; Olafsen, A.; Vistad, O. B.; Roots, J.; Norby, P. *J. Mater. Chem.* **2005**, *15*, 4695.
13. Gursky, J. A.; Blough, S. D.; Luna, C.; Gomez, C.; Luevano, A. N.; Gardner, E. A. *J. Am. Chem. Soc.* **2006**, *128*, 8376.
14. Hibino, T.; Kobayashi, M. *J. Mater. Chem.* **2005**, *15*, 653.
15. Jaubertie, C.; Holgado, M. J.; San Romaj, M. S.; Rives, V. *Chem. Mater.* **2006**, *18*, 114.
16. Miyata, S. *Clays Clay Minerals* **1983**, *31*, 305.
17. Strawhecker, K. E.; Manias, E. *Chem. Mater.* **2000**, *12*, 2943.
18. Zhao, C. X.; Liu, Y.; Wang, D. Y.; Wang, D. L.; Wang, Y. Z. *Polym. Degrad. Stab.* **2008**, *93*, 1323.
19. Marangoni, R.; Mikowski, A.; Wypych, F. *J. Colloid Interface Sci.* **2010**, *351*, 384.
20. Ramaraj, B.; Sanjay, K. S.; Yoon, K. R. *J. Appl. Polym. Sci.* **2010**, *116*, 1671.
21. Huang, S.; Cen, X.; Zhu, H.; Yang, Z.; Yang, Y.; Tjiu, W. W.; Liu, T. *Mater. Chem. Phys.* **2011**, *130*, 890.
22. Gaume, J.; Rivaton, A.; Therias, S.; Gardette, J. L. *Polym. Degrad. Stab.* **2012**, *97*, 488.
23. Lemaire, J.; Arnaud, R.; Gardette, J. L. *Revue Générale des Caoutchoucs et Plastiques* **1981**, *613*, 87.
24. Inayat, A.; Klumpp, M.; Schwieger, W. *Appl. Clay Sci.* **2011**, *51*, 452.
25. Zhou, Q.; Verney, V.; Commereuc, S.; Chin, I. J.; Leroux, F. *J. Colloid Interface Sci.* **2012**, *349*, 127.
26. Gaume, J.; Wong-Wah-Chung, P.; Rivaton, A.; Therias, S.; Gardette, J. L. *RSC Adv.* **2011**, *1*, 1471.
27. Lonkar, S. P.; Therias, S.; Caperaa, N.; Leroux, F.; Gardette, J. L.; *Eur. Polym. J.* **2010**, *46*, 1456.
28. Bocchini, S.; Morlat-Therias, S.; Gardette, J. L.; Camino, G. *Eur. Polym. J.* **2008**, *44*, 3473.
29. Morlat, S.; Mailhot, B.; Gonzalez, D.; Gardette, J. L. *Chem. Mater.* **2004**, *16*, 377.